H1prelim-14-013 Submitted to

XXII International Workshop on Deep-Inelastic Scattering and Related Subjects, DIS2014, April 28 – May 2, 2014, Warsaw, Poland
Parallel Session **Small-x, Diffraction and Vector Mesons**

Electronic Access: www-h1.desy.de/publications/H1preliminary.short list.html

Dijet Production with Large Rapidity Gap in Diffractive Deep-inelastic Scattering at HERA

H1 Collaboration

Abstract

In this measurement, the cross section for dijet production in diffractive deep-inelastic scattering is presented. The diffractive events are selected by requiring the presence of a Large Rapidity Gap in the forward region of the H1 detector. The data have been collected during the HERA-II period and correspond to an integrated luminosity of 284 pb^{-1}. The data cover the range $4 < Q^2 < 80\ \mathrm{GeV}^2$ in photon virtuality. The phase space of the analysis is defined by two inclusive jets found by the k_T cluster algorithm in the hadronic centre-of-mass system. The leading and sub-leading jets are required to have $p^*_{T,1} > 5.5\ \mathrm{GeV}^2$ and $p^*_{T,2} > 4.0\ \mathrm{GeV}^2$, respectively and to lie within the pseudorapidity range $-1 < \eta_{1,2} < 2$. The phase space of the measurement is specified in detail in Table 1. Differential cross sections are compared to QCD Next-to-leading order calculations based on diffractive parton distribution functions extracted in inclusive diffractive measurements.

$4 < Q^2 < 80\ \mathrm{GeV}^2$
$0.1 < y < 0.7$
$p^*_{T,1} > 5.5\ \mathrm{GeV}$
$p^*_{T,2} > 4.0\ \mathrm{GeV}$
$-1 < \eta_{1,2} < 2$
$x_{I\!P} < 0.03$
$\lvert t \rvert < 1\ \mathrm{GeV}^2$
$M_Y < 1.6\ \mathrm{GeV}$

Table 1: Phase space of the diffractive DIS dijet measurement.

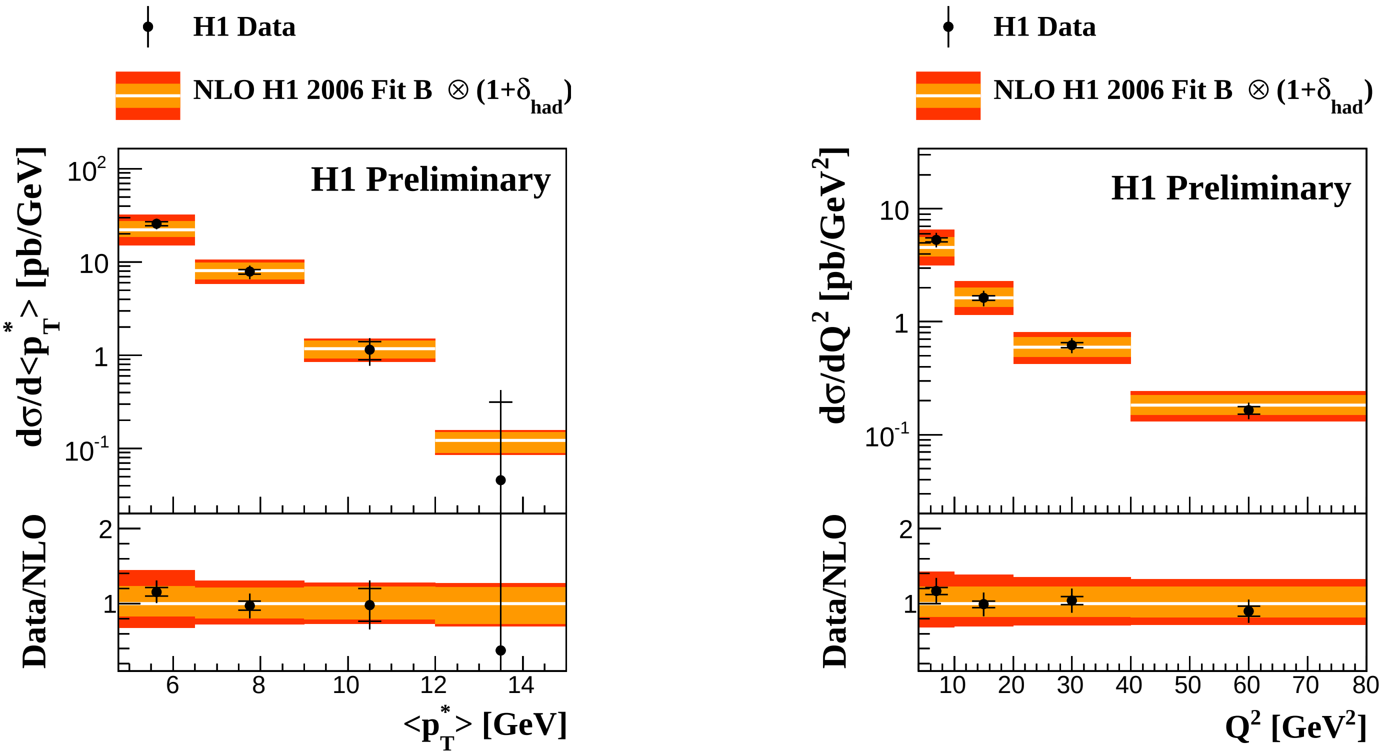

Figure 1: Diffractive dijet differential cross section as a function of $\langle p_T^* \rangle$ and Q^2. The inner error bars of the data points represent the statistical uncertainty while the outer error bars include the systematic uncertainties added in square. The NLO QCD prediction based on the DPDF set H1 2006 B is displayed as the white line with the inner band (orange) indicating the uncertainty of hadronization and DPDF fit added in square. The outer band (red) includes the QCD scale uncertainty.

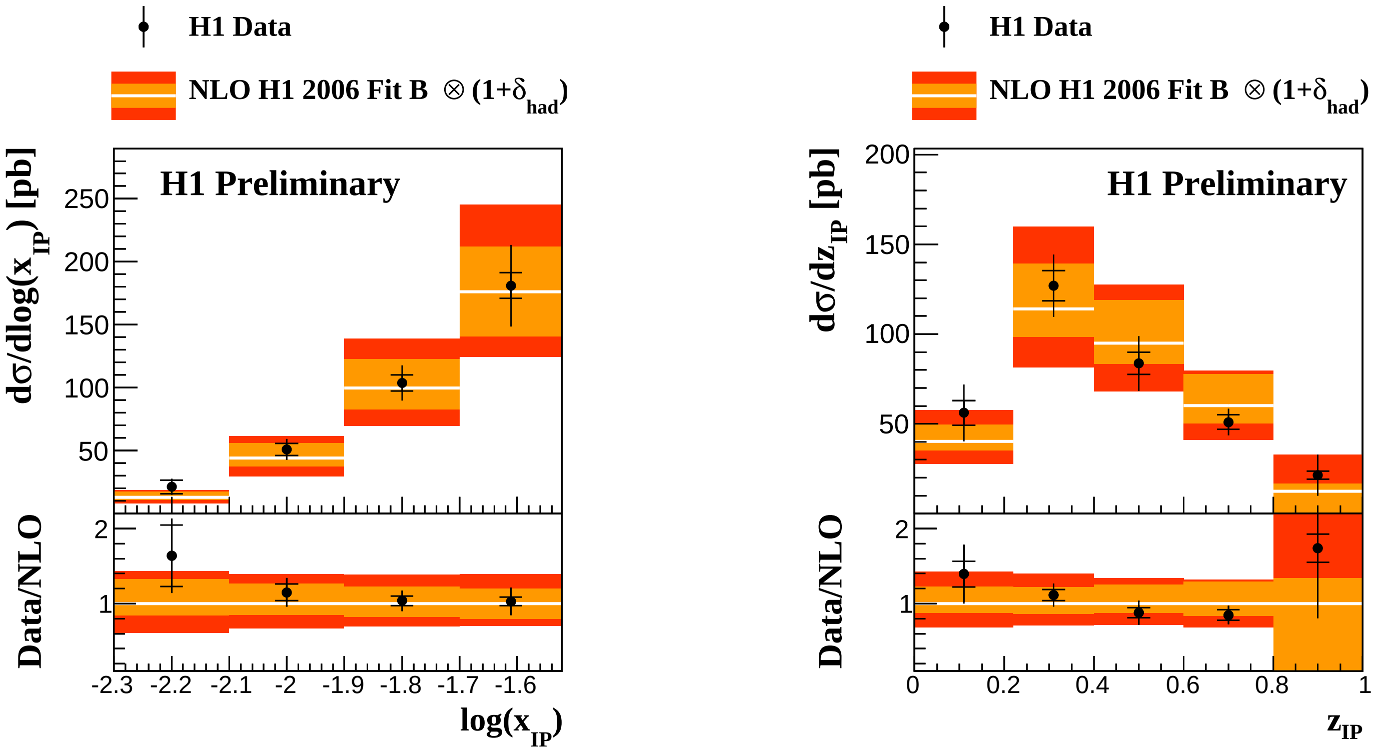

Figure 2: Diffractive dijet differential cross section as a function of $\log(x_{I\!P})$ and $z_{I\!P}$. The inner error bars of the data points represent the statistical uncertainty while the outer error bars include the systematic uncertainties added in square. The NLO QCD prediction based on the DPDF set H1 2006 B is displayed as the white line with the inner band (orange) indicating the uncertainty of hadronization and DPDF fit added in square. The outer band (red) includes the QCD scale uncertainty.

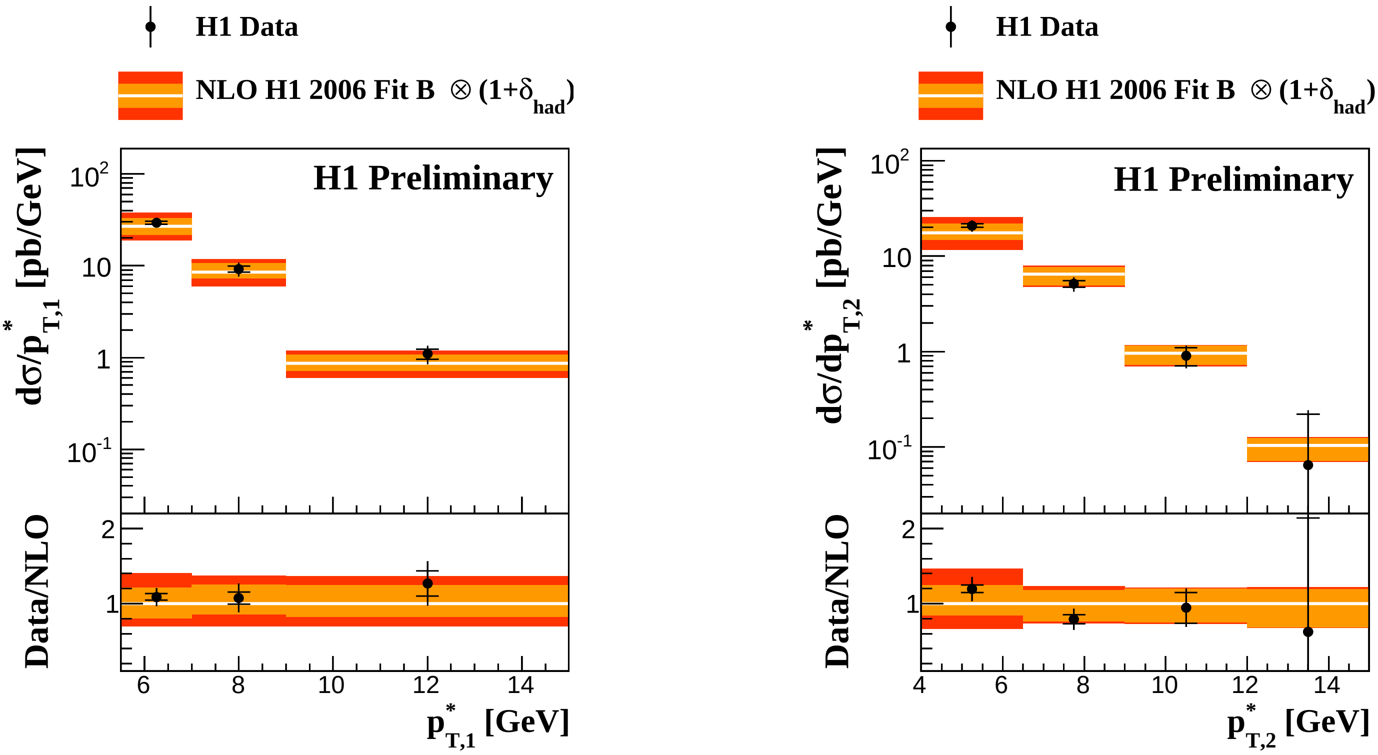

Figure 3: Diffractive dijet differential cross section as a function of $p^*_{T,1}$ and $p^*_{T,2}$. The inner error bars of the data points represent the statistical uncertainty while the outer error bars include the systematic uncertainties added in square. The NLO QCD prediction based on the DPDF set H1 2006 B is displayed as the white line with the inner band (orange) indicating the uncertainty of hadronization and DPDF fit added in square. The outer band (red) includes the QCD scale uncertainty.

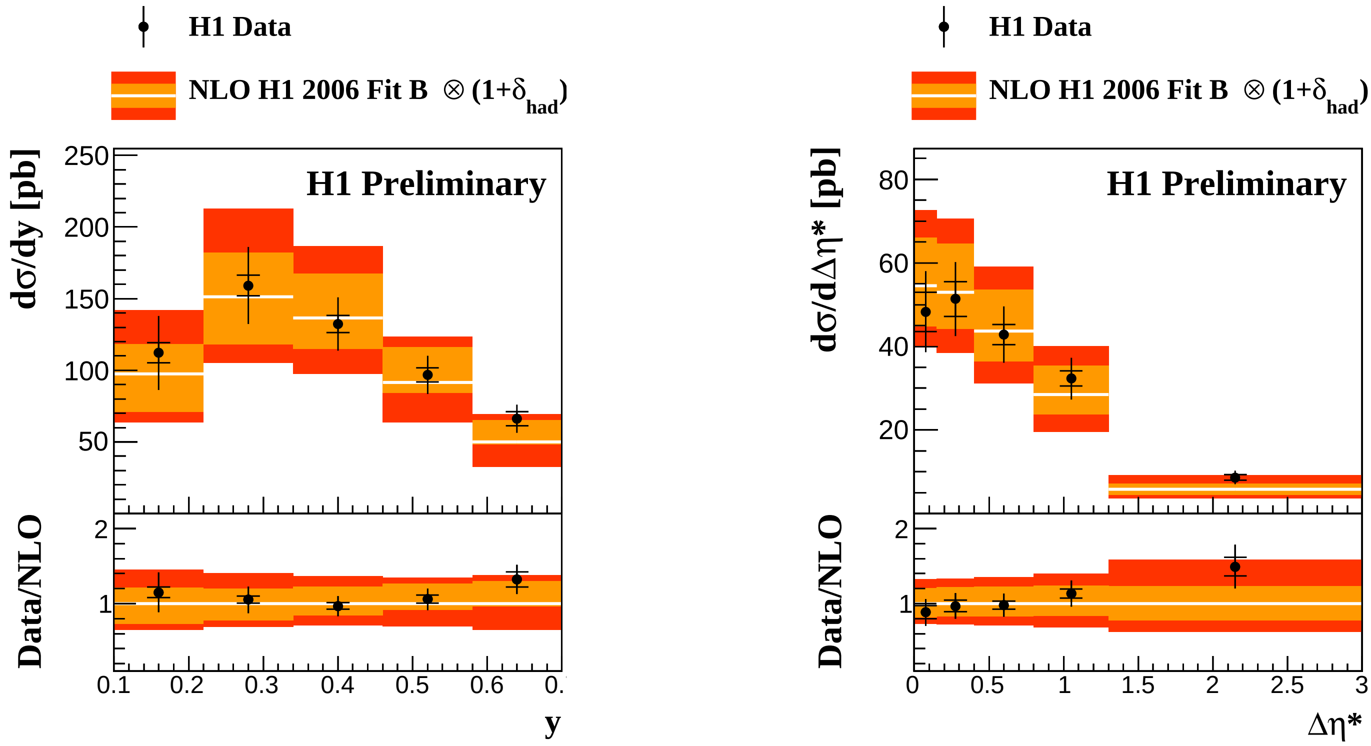

Figure 4: Diffractive dijet differential cross section as a function of y and $\Delta\eta^* = |\eta_1^* - \eta_2^*|$. The inner error bars of the data points represent the statistical uncertainty while the outer error bars include the systematic uncertainties added in square. The NLO QCD prediction based on the DPDF set H1 2006 B is displayed as the white line with the inner band (orange) indicating the uncertainty of hadronization and DPDF fit added in square. The outer band (red) includes the QCD scale uncertainty.